

## Precise Measurement of the Static Electric-Field Ionization Rate for Resolved Hydrogen Stark Substates

Peter M. Koch

*Laboratoire de Physique de l'École Normale Supérieure, 75231 Paris Cedex 05, France,<sup>(a)</sup> and  
J. W. Gibbs Laboratory, Yale University, New Haven, Connecticut 06511<sup>(b)</sup>*

and

David R. Mariani

*J. W. Gibbs Laboratory, Yale University, New Haven, Connecticut 06511*

(Received 24 November 1980)

We report the first precise measurements of the ionization rate  $\Gamma_I(\mathbf{F})$  in the tunneling regime for resolved  $n=30, 40$  Stark substates of hydrogen. Excellent agreement is obtained with nonrelativistic numerical calculations. No effects of wave function mixing induced by relativistic or other interactions were observed. We consider and give an experimental upper limit for the magnitude of the H-D isotopic shift in  $\Gamma_I(\mathbf{F})$ .

PACS numbers: 32.60.+i, 35.10.-d

Fifty years ago, Rausch von Traubenberg, Gebauer, and Lewin<sup>1</sup> observed the electric quenching of the ( $n=4-8$ ) hydrogen Balmer lines, but the resolution of their spectrograms was too low to permit a measurement of the actual electric field dependence of an ionization rate  $\Gamma_I(F)$ . This Letter reports the first precise, absolute measurement of  $\Gamma_I(F)$  for individual substates labeled by parabolic quantum numbers<sup>2</sup>  $\{n, n_1, n_2, |m|\}$ , where  $n=n_1+n_2+|m|+1$ . One of us has previously measured precisely<sup>3</sup> the real part of the complex energy  $E(F)=E_R(F)-i\Gamma_I(F)/2$  used for a Breit-Wigner description of these resonances. The recent renaissance of theory<sup>2,4-6</sup> for the nonrelativistic, spinless approximation has emphasized its mathematics as well as analytic and numerical calculations of  $E_R(F)$  and  $\Gamma_I(F)$ .

The experiment used a fast beam ( $>8$  keV) of H atoms drifting at constant speed (measured to  $\Delta v/v \approx 0.2\%$ ) through five magnetically shielded,<sup>3</sup> equal-polarity, transverse electric fields  $F_i$ ,  $i=1-5$ . Previously described<sup>7</sup> collinear, cw  $^{12}\text{C}^{16}\text{O}_2$  laser ( $5-20$  W/cm<sup>2</sup>) excitation methods were used (see especially Fig. 1 of Ref. 7) to prepare in 8.26(16)-cm-long  $F_3$  atoms in individual Stark substates of  $n=30$  or 40 ( $\sim 10^{5-7}$ /cm<sup>2</sup> sec). A 1.9-cm-long  $F_4 \approx 100$  V/cm avoided loss of substate definition in a low- $F$  region<sup>3,7</sup> as these atoms drifted adiabatically into the ionization field  $F_5$  between  $L_5=8.26(16)$ -cm-long, 7.6-cm-high Au-plated Cu parallel plates whose average separation  $d_5=0.9436(10)$  cm was measured with a spectroscopic method.<sup>7</sup> Those atoms surviving passage through the entrance fringe field, constant  $F_5$  in the middle, and exit fringe field were detected<sup>3</sup> by microwave multiphoton ionization in

a voltage-labeled cavity and analog detection ( $\sim 3$  ms time constant) of the resultant energy-labeled protons with a Johnston MM1 particle multiplier, a field-effect transistor op-amp electrometer, a PAR HR-8 lockin amplifier, and a voltage-to-frequency converter. Quench curves similar to Fig. 1 were accumulated for each substate as a function of  $F_5$  in a 512-channel multiscaler (7 ms/channel dwell time) synchronized to the repetitive ( $\frac{1}{4}$  Hz) sweep of the applied potential difference  $V_5$ . Since experimental tests or calculations showed that radiative processes, both spontaneous<sup>8</sup> and 300 °K blackbody photon induced,<sup>9</sup> and

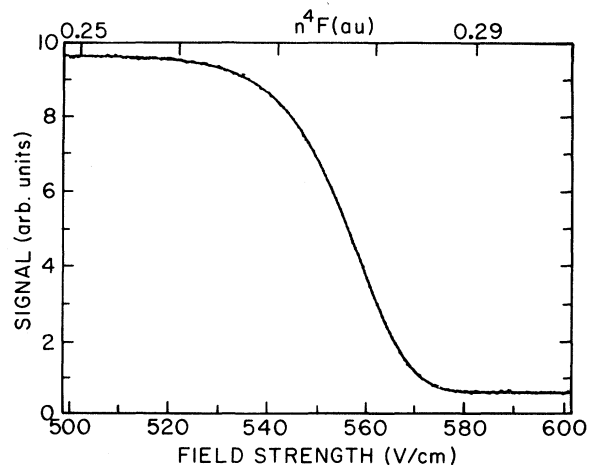


FIG. 1. The surviving intensity of atoms in the substate  $\{40, 39, 0, 0\}$  as a function of  $F$  or  $n^4 F$  (a.u.). The base line was shifted by an intentional instrumental offset. The raw data (dots) are obscured by a least-squares fit.

collision processes<sup>10</sup> in the  $\approx 10^{-7}$  Torr apparatus vacuum had a negligible influence, we assumed that each curve represented only ionization.

Observations with Na Rydberg atoms of non-monotonic static- $F$  dependence of  $\Gamma_I(F)$ <sup>11</sup> and of both adiabatic (or "saddle-point"<sup>2</sup>) and diabatic (hydrogenic) ionization thresholds in a time-slewed  $F$ <sup>12</sup> have been explained by wave function mixing at avoided crossings of equal- $|m|$  levels. The spherically symmetric core ion potential breaks a dynamical symmetry<sup>2,13</sup> of the Schrödinger equation for the pure Coulomb-Stark potential  $V(r) = -r^{-1} + Fz$ , whose substates theoretically cross exactly.<sup>14</sup> In hydrogen, where this symmetry is broken predominantly by relativistic interactions, calculations<sup>15</sup> within each of the  $n = 2-4$  manifolds do show avoided crossings of equal- $|m_j|$  levels, but no calculation of *inter-n-manifold* avoided crossings and their effect on ionization has been reported. That each presently studied H substate had a *monotonic* ionization curve similar to Fig. 1, with constant asymptotes joined by a *single* smooth drop at a range of  $F_5$  expected for pure tunneling (i.e., far above the saddle-point threshold<sup>2</sup>  $n^4F \approx \frac{1}{16}$  a.u. and near but below its classical threshold value<sup>16</sup> of  $n^4F$ ), is consistent with diabatic traversals<sup>12</sup> of avoided crossings in the fringe fields of  $F_5$  (time slewed

at  $\sim 10^8$  V/cm sec in the atom rest frame) and with negligible ( $\approx 5 \times 10^5$  s<sup>-1</sup>) ionization induced by wave function mixing<sup>11</sup> during the  $\sim 6 \times 10^{-8}$  sec of constant  $F_5$  when the  $n = 40$  substates of Fig. 2 were degenerate with the continuum of rapidly ionizing levels in higher manifolds.

To account systematically for the fringe fields in the data reduction, we performed with a DEC-10 computer a seven-parameter, nonlinear least-squares fit<sup>17</sup> to each ionization curve ( $\approx 150$  channels of data) using the exponential decay trial function

$$S(F) = S_1 \exp\left[-\int \Gamma_I(F_5(x)) dx/v\right] + S_0.$$

The integrand gives the probability of ionization during a differential time period  $dx/v$  in a field  $F_5(x)$  evaluated at a point  $x$  along the beamline;  $S_1 + S_0$  and  $S_0$  are, respectively, the fitted values of the upper and lower asymptotes. The nonzero value of  $S_0$  was produced by an intentional constant zero offset on the lock-in amplifier. Since it accurately reproduced theoretical  $\ln \Gamma_I$  vs  $F$  curves (Figs. 2 and 3; see also Ref. 6), we modeled  $\Gamma_I(F)$  with the exponential function of a fourth-order polynomial in  $F$  (five parameters,  $P_1-P_5$ ). The numerical integration of the fit through each fringe field<sup>18</sup> was terminated with negligible error when  $F_5(x)/F_5(\text{center of electrodes}) < 0.3$ .

The fitted curve in Fig. 1 covers the  $\approx 150$  raw data points well, showing that the fitting procedure accurately reproduced the shape of the experimental curves. The parameters  $P_1-P_5$  found

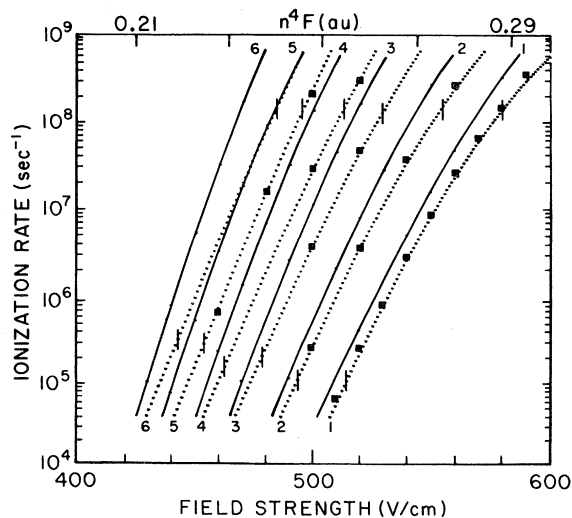


FIG. 2. Dotted lines, experimental  $\Gamma_I(F)$  curves for the substates 1:  $\{40, 39, 0, 0\}$ ; 2:  $\{40, 38, 0, 1\}$ ; 3:  $\{40, 38, 1, 0\}$ ; 4:  $\{40, 37, 1, 1\}$ ; 5:  $\{40, 37, 2, 0\}$ ; 6:  $\{40, 36, 2, 1\}$ . The tic marks are explained in the text. Solid lines, theoretical curves calculated with Eq. (6) of Ref. 6. Squares, numerical theoretical results (Ref. 19).

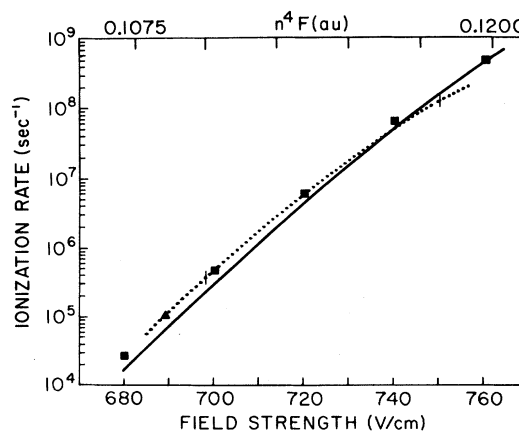


FIG. 3. Dotted line, experimental  $\Gamma_I(F)$  curve for the substate  $\{30, 0, 29, 0\}$ . The tic marks are explained in the text. Solid line, theoretical curve calculated with Eq. (6) of Ref. 6. Numerical theoretical results are shown as squares (Ref. 19) and triangle (Ref. 2).

by each fit were used to plot the dotted experimental  $\Gamma_I(F)$  curves in Figs. 2 and 3. Vertical tic marks bound the experimentally significant portion of each curve; in the best cases, the dynamic range is  $>10^3$ . Above (below) each upper (lower) tic mark, where each fitted ionization curve approached within one standard deviation of the raw data in the lower (upper) asymptote, the experiment gave only a lower (upper) bound for  $\Gamma_I(F)$ . Well inside the tic marks, approximately where  $10^6 \text{ s}^{-1} \leq \Gamma_I(F) < 10^8 \text{ s}^{-1}$ , the probable error caused by noise in the data is smaller than the  $\sim \pm 15\%$  uncertainty in  $\Gamma_I(F)$  caused by the estimated  $\pm 0.2\%$  experimental uncertainty in  $F_5$ . By comparison, quoted uncertainties in  $L_5$  and  $v$  produced negligible errors. Less accurate analysis without a fit produced  $\Gamma_I(F)$  curves in agreement with the parametric curves, but the point-by-point fluctuations near the tic marks were huge.

In Figs. 2 and 3 the squares are the results of "numerically exact" calculations<sup>19</sup> kindly performed by Damburg and Kolosov (DK), who used an infinite nuclear mass. The triangle in Fig. 3 is a numerical result of Luc-Koenig and Bachelier<sup>2</sup> (LKB), apparently with the reduced-mass scaling for hydrogen effected but with a slightly incorrect<sup>2</sup> atomic unit of  $F$ . We estimate that use of the correct value<sup>2</sup> would lower their point by  $\sim 1\%$ , making it agree within  $1\%$  with a curve that we fitted through the squares. This seems to imply that reduced-mass corrections shift  $\Gamma_I(F) \approx 1\%$ , a point we question below.

With one exception these theoretical results deviate from the portions of the experimental  $\Gamma_I(F)$  curves between the tic marks by an amount ( $<15\%$ ) less than the experimental uncertainty. This excellent agreement shows that nonrelativistic numerical theory accurately predicts  $\Gamma_I(F)$  for the present range of  $n$  and  $F$ .

The small discrepancy in Fig. 3 near 740 V/cm could be explained by our laser-excitation<sup>7</sup> method producing an unwanted  $\approx 3\%$  admixture in the beam of higher-lying  $n=30$  substate(s) which ionized at higher  $F$  than did  $\{30, 0, 29, 0\}$ . Tests and calculations lead us to believe that this source of systematic error did not appreciably affect our  $n=40$  data, however.

The solid curves in Figs. 2 and 3 were calculated using the asymptotic formula of Damburg and Kolosov, Eq. (6) of Ref. 6. For  $E_R(F)$ , we used the more accurate Padé approximant<sup>20</sup>  $[2/2]$  rather than fourth-order perturbation theory. We found that use of reduced-mass corrections for

$F$  and  $E_R(F)$  (Ref. 2, p. 1756) significantly affected the calculated results. Relative to those for an infinite nuclear mass, the calculated curves for the  $n=40$  H substates in Fig. 2 and  $n=30$  H substate in Fig. 3 increased by about  $6\%$ – $9\%$  and  $8\%$ – $11\%$ , respectively. Since the latter shift is inconsistent with the agreement noted above for the LKB and DK numerical results, the use of reduced-mass corrections in numerical and analytic calculations of  $\Gamma_I(F)$  needs further attention. The analytic curves in Fig. 2 disagree with experimental and numerical results by a factor which increases from about 2 to 10 as  $n_1 - n_2$  decreases from 39 to 34. In Fig. 3, the discrepancy is less than or approximately equal to a factor of 2. It would be useful to have more accurate formulas.

We attempted a direct relative measurement of the H-D isotope effect for  $\{40, 39, 0, 0\}$ . Ionization curves like Fig. 1 (four for each isotope) were alternately recorded separately for H and D beams traveling at the same (within  $0.2\%$ ) velocity  $v/c = 4.17 \times 10^{-3}$  and experiencing the same  $F_5$  sweep. An analysis based on channel-by-channel subtraction of different H-D, H-H, and D-D pairs of curves gave a  $3\%$  upper limit for the H-D difference in  $\Gamma_I(F) \sim 10^7 \text{ s}^{-1}$  at fixed  $F$ . This can be compared to the  $\sim 3\%$  effect we calculated with the DK formula. With improvements to our apparatus, we should be able to achieve  $1\%$  relative precision.

Future experiments should investigate symmetry-breaking effects at much lower  $n$  values, predicted crossing of  $\Gamma_I(F)$  curves,<sup>6</sup> measurements of large  $\Gamma_I(F) \geq 10^{11} \text{ s}^{-1}$  where different numerical calculations disagree (Ref. 2, Table I), and photoabsorption resonances<sup>2</sup> near the  $E=0$  limit. It would also be possible to measure precisely the ionization of singlet and triplet Rydberg states of He,<sup>21</sup> the simplest multielectron atom.

This research was supported by the National Science Foundation under Grant No. PHY-78-25655. We thank R. Damburg and V. Kolosov for performing requested calculations. One of us (P.M.K.) acknowledges the support of A. P. Sloan and Yale Junior Faculty Fellowships and the hospitality of S. Haroche and the other members of Laboratoire de Spectroscopie Hertzienne de l'École Normale Supérieure, where this paper was written.

<sup>(a)</sup>Address until 1 August 1981.

<sup>(b)</sup>Permanent address.

<sup>1</sup>H. Rausch v. Trautenberg, R. Gebauer, and G. Lewin, *Naturwissenschaften* **18**, 417 (1930).

<sup>2</sup>E. Luc-Koenig and A. Bachelier, *J. Phys. B* **13**, 1743, 1769 (1980). We find their atomic unit of  $F$  to be in error. The correct value is  $5.142250(17) \times 10^9$  V/cm based on the fundamental constants given by E. R. Cohen and B. N. Taylor, *J. Phys. Chem. Ref. Data* **2**, 663 (1973).

<sup>3</sup>P. M. Koch, *Phys. Rev. Lett.* **41**, 99 (1978). A small error made by that author in the Raleigh-Schrödinger perturbation-theory calculation of the wave numbers of each  $\{L\}$  state necessitates a slight revision of the measured wave numbers for the  $\{U\}$  states given there in Figs. 3 and 4. The corrected wave numbers are  $-109.369(14)$   $\text{cm}^{-1}$  for  $\{25, 21, 2, 1\}$  and  $-163.950(7)$   $\text{cm}^{-1}$  for  $\{30, 0, 29, 0\}$ . No conclusions of that paper are affected.

<sup>4</sup>L. Benassi, V. Grecchi, E. Harrell, and B. Simon, *Phys. Rev. Lett.* **42**, 704 (1979); L. Benassi and V. Grecchi, *J. Phys. B* **13**, 911 (1980).

<sup>5</sup>H. J. Silverstone, B. G. Adams, J. Cizek, and P. Otto, *Phys. Rev. Lett.* **43**, 1498 (1979).

<sup>6</sup>R. J. Damburg and V. V. Kolosov, *J. Phys. B* **12**, 2637 (1979), and references therein.

<sup>7</sup>P. M. Koch and D. R. Mariani, *J. Phys. B* **13**, L645 (1980).

<sup>8</sup>J. R. Hiskes, C. B. Tarter, and D. A. Moody, *Phys. Rev.* **133**, A424 (1964).

<sup>9</sup>J. W. Farley and W. H. Wing, *Phys. Rev. A* **23**, 2397 (1981).

<sup>10</sup>P. M. Koch, *Phys. Rev. Lett.* **43**, 432 (1979).

<sup>11</sup>M. G. Littman, M. L. Zimmerman, and D. Kleppner, *Phys. Rev. Lett.* **37**, 486 (1976).

<sup>12</sup>T. H. Jeys, G. W. Foltz, K. A. Smith, E. J. Beiting, F. G. Kellert, F. B. Dunning, and R. F. Stebbings, *Phys. Rev. Lett.* **44**, 390 (1980).

<sup>13</sup>K. Helfrich, *Theor. Chim. Acta* **24**, 271 (1972).

<sup>14</sup>It is easy to show that all avoided crossings predicted by G. J. Hatton, *Phys. Rev. A* **16**, 1347 (1977), occur far above the highest classical ionization threshold  $n^4 F_c \approx 0.38$  a.u. [D. Banks and J. G. Leopold, *J. Phys. B* **11**, 37 (1978)], where the widths of the states would be huge.

<sup>15</sup>G. Lüders, *Ann. Phys. (Leipzig)*, **8**, 301 (1951).

<sup>16</sup>Banks and Leopold, Ref. 14.

<sup>17</sup>P. R. Bevington, *Data Reduction and Error Analysis for the Physical Sciences* (McGraw-Hill, New York, 1969).

<sup>18</sup>R. G. E. Hutter, *J. Appl. Phys.* **18**, 797 (1947).

<sup>19</sup>R. J. Damburg and V. V. Kolosov, *J. Phys. B* **9**, 3149 (1976), and private communication.

<sup>20</sup>H. J. Silverstone and P. M. Koch, *J. Phys. B* **12**, L537 (1979).

<sup>21</sup>P. M. Koch, *Opt. Commun.* **20**, 115 (1977).

## Angular Distribution of Photoelectrons in Strongly Driven Multiphoton Transitions

S. N. Dixit and P. Lambropoulos

*Department of Physics, University of Southern California, Los Angeles, California 90007*

(Received 6 February 1981)

The behavior of photoelectron angular distributions in a strongly driven resonant multiphoton ionization process is discussed. It is shown that the angular distribution changes drastically with increasing intensity as a result of the ac Stark shifting of the levels. Moreover, under strong saturation conditions the distribution reaches a limiting form significantly different from the form predicted by perturbation theory. The effects of the laser bandwidth on the angular distribution are also discussed briefly.

PACS numbers: 32.80.Kf, 32.80.Fb

Recent experimental studies<sup>1-3</sup> of photoelectron angular distributions and spin polarization point to the increasing sophistication with which such measurements are employed as spectroscopic tools. It has become feasible to obtain rather detailed experimental information about excited states through selective excitation. Moreover, ionization of selectively excited states is an extremely sensitive method for determination of their properties. It is generally assumed that strong intensity effects complicate the picture and are to be avoided if possible. Desirable as it may be, it is not always possible as in many instances the strong intensity is the very condition that makes the process observable. Recent

theoretical studies of related resonant multiphoton processes<sup>4-6</sup> have revealed a number of subtle features due to the effects of laser intensity, its bandwidth and line shape, and in some cases its complete coherence properties. A rigorous theory incorporating these features can be developed for extracting values for atomic parameters such as matrix elements, phase shifts, spin-orbit coupling, etc. In a most recent case study, we have shown by a rigorous treatment that the influence of such effects on the spin polarization of the photoelectron is quite significant.<sup>7</sup> In this Letter we report certain unusual and surprising results on some of the basic aspects of angular distributions. We show that the